AUTHOR(S): FAISAL, N.H., AHMED, R., GOEL, S. and CROSS, G.

TITLE: Future of nanoindentation in archaeometry.

YEAR: 2018

Publisher citation: FAISAL, N.H., AHMED, R., GOEL, S. and CROSS, G. 2018. Future of nanoindentation in archaeometry. Journal of materials research [online], 33(17), pages 2515-2532. Available from: https://doi.org/10.1557/jmr.2018.280

OpenAIR citation: FAISAL, N.H., AHMED, R., GOEL, S. and CROSS, G. 2018. Future of nanoindentation in archaeometry. Journal of materials research, 33(17), pages 2515-2532. Held on OpenAIR [online]. Available from: https://openair.rgu.ac.uk

Future of nanoindentation in archaeometry

Nadimul Haque Faisal[a,1], Rehan Ahmed[b], Saurav Goel[c], Graham Cross[d,e]

[a] *School of Engineering, Robert Gordon University, Garthdee Road, Aberdeen, AB10 7GJ, UK*

[b] *School of Engineering and Physical Sciences, Heriot-Watt University, Edinburgh, EH14 4AS, UK*

[c] *School of Aerospace, Transport and Manufacturing, Cranfield University, Cranfield, MK43 0AL, UK*

[d]*Adama Innovations Limited, Dublin 2, Ireland*

[e]*CRANN Nanoscience Institute, School of Physics, Trinity College, Dublin 2, Ireland*

Abstract

This review aims to consolidate a scattered literature on the use of a modern nanomechanical testing techniques in archaeometry materials research such as the process of mummification. It is concluded that nanoindentation tests can provide valuable data about mechanical properties which, in turn, relate to the evolution of ancient biomaterials as well as human history and production methods. As an emerging novel application of an existing technique, some special considerations are warranted for characterization of archaeometry materials. In this review, potential research areas relating to how nanoindentation is expected to benefit and help improve existing practices in archaeometry are identified. These probe new insights into the field and will hopefully raise awareness for use of nanoindentation in world heritage sites.

Keywords: *nanoindentation, micromechanics, archaeometry, structure-property relationships.*

[1] Corresponding authors. E-mail addresses: N.H.Faisal@rgu.ac.uk; Tel: +44 (0) 1224-26 2438.

1. INTRODUCTION

Inspection of archaeological materials (e.g. metals, paints, claws, teeth, stones, bones, skins, etc.) is often an intricate task due to fabrication history, the composite chemical and structural alterations that are caused by the alloying, annealing, and working processes of production, as well as by post-manufactured conditions. For centuries, archaeologists have been seeking to use analytical methods that can yield detailed quantitative and accurate interpretations about the prehistoric past. The analysis of archaeological objects necessitates investigators to address the problem, by knowing features like grain size (i.e. microstructure) and other measurable characteristics of the item. A natural question arises: Is it is possible to go backwards to obtain insight into the forming conditions or production processes? [1]. Therefore, the principle motivations and applications of nanomechanical testing (nanoindentation) to archaeological materials would be understanding ancient manufacturing, storage, and usage processes by characterization of microstructure, and doing the above within small test volumes in small, rare and/or potentially priceless samples. A potential for ageing studies exists also exists for the technique, however these remain much less developed to date.

Nanoindentation (ISO 14577 [2] and ASTM E2546–07 [3]) is a technique with high spatial resolution to precisely characterize and probe the mechanical behaviour of materials [4]. The technique is applied widely in the areas of aerospace, energy, electronics, and healthcare, and deals with a range of materials like carbon fibre reinforced polymer (CFRP), carbon materials, coatings and alloys, civil engineering and polymeric materials, organic feedstock materials in bioenergy area and semiconductor materials like silicon to probe useful properties like hardness, modulus, fracture toughness, wear resistance, coefficient of friction, creep, visco-elasticity and interfacial bond strength. It has precedence in historical contexts as well, being used recently, for example, to analyse dental wear mechanics in Hadrosaurid

dinosaur samples [5]. The importance of instrumented nanoindentation in the field of archaeometry stems from the fact that the microstructure and surface mechanical properties of materials can help archaeologists to determine the settings under which they were fabricated, used and stored. Studying and probing the process of mummification (shown in **Fig. 1,** indentation zone encircled) [6] dating back to 50 centuries ago is by far the best example of putting nanoindentation in practice.

An understanding of microstructure is a pathway to examine the methods and the degree of control available to ancient manufacturing processes. Further, the surface nature of nanoindentation can reveal clues about the contact history of samples otherwise invisible to macroscopic mechanical testing: Signatures of rubbing, scraping, crushing, cutting and other abrasive or reforming processes can be revealed in the mechanical signals. Exotic samples obtained from archaeological sites require minimally destructive testing methods. The data produced by nanoindentation complements data from other archaeometry methods; For example, the tandem use of multiple surface characterization techniques such as energy dispersive X-ray spectroscopy, electron backscatter diffraction, infra-red spectroscopy, optical imaging, Raman spectroscopy, scanning electron microscopy, transmission electron microscopy, X-ray diffraction and X-ray fluorescence, etc. provides access to variables of archaeological material properties and performance that cannot be gathered from other analytical techniques or grain size analyses only. These supplementary characterization techniques provide a basis for interpreting nanoindentation results when they differ from one sample to the next by, for instance, establishing statistical correlations between elastic modulus and the underlying composition of a material. This is especially true when nanoindentation and a complimentary technique are collected at precisely matched sites. Overall, the ability of the nanoindentation technique to quantitatively characterize the mechanical properties of individual microstructures, phases and constituents in bulk

materials at the nanoscale has been critical for making revolutionary advances in materials characterization.

Archaeological samples are interesting sources of study for phenomena such as aging, alloying, carbon dating and other processing techniques from ancient human civilisation and are therefore of technological intellectual curiosity. New areas of research have traditionally been useful to push forward innovative methods in materials characterization; the test case of applying Raman Spectroscopy for characterization of graphene is an ideal example. One of the principle concerns for testing archaeological samples is preservation, placing a high value on minimally invasive or non-destructive techniques. The criterion for this includes not only structural integrity but also ensuring aesthetic quality for museum display etc. is not compromised. As a technique that probes sample volumes of a few cubic microns or less, well below unaided visual detection, nanoindentation offers a way to extract mechanical data while preserving specimens.

It is also the purpose of this review to show that this nanomechanical method can fill an important gap in experimental characterization of materials in archaeometry, whilst also using other methods to supplement the other aspects of this research field including the likes of techniques such as transmission electron and atomic force microscopy. Research in archaeometry incorporating nanoindentation methods has been scarce but appears to be increasing. Examples in metals [1,7-10], minerals [5,11-12], enamels [13-14], claws [15], paints [16], bones [17-18], and skins [6] are now present in the literature. However, a consolidated understanding on the origins and future pathways of how the technique may be used for samples being extracted from precious world heritage archaeological sites as well as the range of existing materials available in museums worldwide is currently missing. This motivates our review, which attempts to demonstrate the uptake of the instrumented nanoindentation technique and its utility in advancing the archaeometry materials research.

2. INDENTATION CONTACT MECHANICS AND MEASUREMENTS

Instrumented indentation or nanoindentation consists of pressing a rigid (typically diamond) probe or indenter of well-known geometry into the surface of the material under investigation and assessing the ensuing deformation via a high-resolution measurement of displacement. Material mechanical properties are determined by analysing the force-displacement-time (*P*-*h*-*t*) plots recorded during indentation [19-20]. Instruments standardly supply sub-microNewton force and sub-nanometer displacement resolution with large dynamic range. On some occasions, microscopic examination of the impression "fingerprint" left by the indenter in the substrate is performed by optical or scanning probe microscopy upon its retraction. Nanoindenters are also available for *in-situ* SEM and TEM observation during mechanical testing.

Mechanics for elastic, visco-elastic, and elastic-plastic constitutive models have been proposed to describe indentation response (stress state and material accommodation) in variety of materials [21-24]. For material with elastic properties, the indentation impression vanishes after unloading cycle, whereas, for material with plastic properties, permanent deformation appears around the indentation. For elastic-plastic ductile materials like many metals, analytical slip-line field models estimate the permanent deformation along available slip-lines based on yield stress criterion (Tresca or von-Mises) [25], while complex materials require advanced constitutive models and numerical simulation. For plastic deformation in isotropic, ductile material, the standard indentation model [22,25-26] assumes material accommodates the indenter volume by an outwardly expanding hydrostatic core. This hydrostatic core provides symmetry of the stress field under the indenter and which governs the development of concentric hemispherical plastic and elastic shells of deformation that surround the contact [27].

It is well known that the mechanical response of viscoelastic materials depends on load magnitude and contact duration, where the indenter continues penetrating the specimen even under constant load. Under standard analysis, these phenomena can lead to errors in the determination of contact depth which appears as a decrease in apparent elastic modulus and hardness with time [28]. The parameters in a model for viscoelastic response are usually determined from the time course of indenter penetration under constant load [28]. However, the displacement will also be influenced by the initial period of load-increase. This can be considered by correction factors.

It is important to note that the depth-sensing capability of modern instrumented indentation was initially combined [29-30] with traditional indentation methods [21] because of the difficulty at small scales to precisely measure the hardness impression projected contact area upon unloading [29]. However, it was soon realized that this capability allowed for a simple means to simultaneously extract the elastic properties of the material [4], which accounts for much of the wide popularity of the technique today. The basic nanoindentation test simultaneously measures both elastic modulus and hardness of small-volume samples. For isotropic materials, the elastic modulus measured is a convolution of Poisson's ratio (ν) and elastic modulus (E), the latter of which is often extracted by assuming a value for the former (most structural materials lie in the 0.3 to 0.4 Poisson ratio regime). The hardness (H) is a semi-intrinsic material property associated with the plastic tensile yield strength (σ) of the material by the empirical Tabor relation ($H=C\sigma$), where the confinement parameter C~3 for metals and ceramics and C~1.5 for glassy polymeric matter [29]. A variety of indentation features and response can also be measured by considering the deviation of force-displacement loading profiles with that of a reference specimen at the same indentation depth or load [30].

The physical quantities measured from the load-displacement (*P-h)* curve relevant for mechanical property and residual stress measurement are: the maximum load (P_{max}), maximum indentation depth (h_{max}), contact depth (h_c), final indentation depth (h_f), contact area (A_c). The Oliver-Pharr model [4] is the most frequently used method to obtain various mechanical properties (e.g. hardness and elastic modulus) during nanoindentation. Traditionally, the residual elastic modulus (E_r) is derived by measuring the initial unloading contact stiffness (S) which is the slope of the first one-third linear part during unloading cycle of the *P-h* curve. We provide a few further key technical details here, for a complete description of nanoindentation procedures and theory (see e.g. [31-35]). The mean indentation contact pressure or hardness, H, is calculated as [4, 33]:

$$H = \frac{P_{max}}{A_c} \qquad (1)$$

where, P_{max} is the maximum indentation force, A_c is the contact area between the indenter and the surface of the material, which is a function of contact depth, h_c, for example:

$$A_c = \pi a^2 = \pi(\tan\alpha)^2 h_c^{\,2} = 24.5 h_c^{\,2} \qquad (2)$$

for an ideal conical indenter, where α is half apex angle.

The contact depth is calculated as [4, 33]:

$$h_c = h_{max} - \omega\frac{P_{max}}{S} \qquad (3)$$

where ω is a geometric parameter (1 for a flat punch indenter, 0.75 for Berkovich rounded indenter, 0.72 for conical indenter). For individual indentation load-displacement, curves are plotted, and hardness and elastic modulus are calculated for each nanoindentation curve with the Oliver-Pharr (O-P) technique:

$$\frac{1}{E_r} = \frac{1-\nu^2}{E} + \frac{1-\nu_i^2}{E_i} \qquad (4)$$

where E_i, ν_i is elastic modulus and Poisson's ratio of the diamond tip. Reduced modulus E_r is calculated from Sneddon equation [36]:

$E_r = (\sqrt{\pi}/2).(S/\sqrt{A}), S = dP/dh$ (5)

where A is the projected area of elastic contact, S is the contact stiffness. In modern instruments, one can also measure the stiffness continuously [37]. A recent advance in nanoindentation is called 4D tomography, whereby the substrate is mapped over its volume (to a certain depth) at a very high indentation speed [38].

3. NANOINDENTATION IN ARCHAEOMETRY MATERIAL ANALYSIS

3.1 Materials and surface preparation

Based on the sample features (soft or hard, hydrated or dehydrated, porous or non-porous solid) and complexity associated with the compaction, deformation, strain-stiffening or fracture mechanics during indentation, it is necessary to consider different sample preparation practices for an appropriate nanoindentation measurement.

Nanoindentation primarily measures the surface properties of localised small-volume samples. Results of nanoindentation tests are highly influenced by the specimen preparation technique, particularly, if the material under investigation is hard, for example bones (hydrated or dehydrated), as recently summarised by Jiroušek (2012) [39], Bushby *et al.* (2004) [40], Granke *et al.* (2014) [41] and Bembey *et al.* (2006) [42], and teeth, as summarised by Nalla *et al.* (2005) [43], and Angker and Swain (2006) [44].

Historically, flat surface preparation for nanoindentation of most of the engineering materials (e.g. metals, ceramics, coatings) has been commonly done through metallurgical precision cutting, mounting (cold/hot), grinding and fine polishing processes. Apart from metals, the exemplar specimens investigated using nanoindentation includes analysis of range of archaeological material types, e.g. teeth, stones, paints, claws, bones, skins, etc. As flatness is key assumption of most analysis techniques, surface preparation can have a marked influence on the repeatability of the nanoindentation measurements results of such precious

archaeological materials. In this case other sample preparation techniques such as microtoming (cutting extremely thin slices of material) and cryo-microtoming developed for microscopy can be valuable. In all cases careful validation of sample flatness by optical, electron, scanned probe or other high-resolution microscopies is critical.

However, one may note that the variation in nanoindentation measurement is particularly true for biological tissue specimens due to the effort of sample fixation. It is also known both for compact and trabecular bone, that hardness and elastic modulus are dependent on the water content. These conditions result in up to 40% difference in measured indentation modulus [39, 42]. In a well described methodology by Bushby *et al.* (2004) [40], preparation of bone samples involved inclusion of wet or dry bone in a non-infiltrating resin and polishing to a flat surface. It is noteworthy that it is difficult to obtain an adequate surface finish on wet bone while maintaining hydration and preventing interaction with the hydrating fluid and collecting high-quality nanoindentation data. Full dehydration of bone tissue results in marked shrinkage, increased stiffness and strength, and reduced toughness. However, bone embedded in polymethylmethacrylate (PMMA) could permit high resolution analysis in scanning electron microscopy and nanoindentation. As mentioned by Riede and Wheeler (2009) [14], each of the molars inspected was tested on the buccal face, the occlusal tips, and in buccal-to-lingual cross-section taken midway between the tip and the gum-line. All test surfaces were prepared using the process (i.e. metallographically, samples were fixed to a lapping stub using polymer and then polished using a lapping fixture with sequentially finer alumina lapping films). Since nanoindentation testing are time-consuming process, in normal practice, the samples are tested in dry conditions to evaluate the properties of biological materials (e.g. bones, skins). Moisture promotes enzymatic deprivation of such biological materials (e.g. bones, skins), the bone collagen matrix and because the nanomechanical tests with large set of different test constraints take longer times, it would be very tough to

preserve or sustain the test conditions during the experiments. For all these reasons, biological specimens to be tested are normally dried in stable conditions prior to the experiments, as it has been revealed through numerous investigations that the stiffness is generally complex (higher) than stiffness of the bone samples tested under wet conditions [39, 42].

In an example of sample preparation for indentation of skin, Janko *et al.* (2010) [6] obtained histological specimens and 2 µm to 4 µm thick transverse (crosswise) sections were cut and transferred onto transparent slides. To prepare the histological sections, new skin samples were exposed to the same procedures as the mummified tissue. As a reference, Janko *et al.* (2010) [6] used an analogous recent human skin sample that was taken from a volunteer for indentation analysis. Jiroušek (2012) [39] have highlighted the work of Dudíková *et al.* (2011) [45] relating optimisation of the sample preparation process, where the effects of the grain size, load and duration time of polishing on surface unevenness were analysed using laser scanning microscopy (e.g. confocal type). There is other research on modern skin samples by Bhushan and Tang (2010) [46] where the samples were mounted on the AFM and the nanoindenter sample pucks with a rapid drying glue, a method which is generally not implemented across all material types. In a work by Crichton *et al.* (2013) [47], the skin sample was mounted onto a stainless-steel stage with double-sided tape, and filter paper soaked in saline was placed in contact with the excision surface to ensure that the tissue did not dehydrate (possibly to maintain structural integrity of sample to an extent) from these surfaces during experimentation.

3.2 Measurement and characterization

3.2.1 Metals

The extant literature provides examples of ancient metals that have been analysed using nanoindentation techniques. Changes within the structure of the metal could be identified which would identify microstructurally age-related modifications, to help determine the tempering processes involved, type of original material used and the composition of the metal [7,9]. For example, nanoindentation investigation has been done by Northover *et al.* (2013) [7] on eutectic Ag-Cu alloys from archaeological and historical contexts to examine the hardness dissimilarity in the transformed region. As suggested, this has been of curiosity since age-related variations at grain boundaries were first proposed as an indicator of antiquity and authenticity. A second strand of interest proposed by Northover *et al.* (2013) [7] has been the embrittlement of archaeological silver by isolation of impurities to grain boundaries. To understand the microstructures of archaeological silver the important interrogation is how to differentiate between the respective contributions of manufacture, age and environment. The eutectic Ag-Cu system can display a variety of precipitate morphologies and these can be characterized using nanoindentation. The hardness results given by Northover *et al.* (2013) [7] are those measured during unloading. **Figure 2(a)** shows a line of indentations made across a transformed region and into an untransformed region on each side. The hardness plot (**Fig. 2(b)**) shows a modification in hardness across the altered region which suggest a steady change in the coarseness of precipitation.

In an investigation by Patzke *et al.* (2008) [8] and Reibold *et al.* (2006) [48] on how Damascene blades (showing unexpected mechanical and optical features) were manufactured following secret recipes, there were signs that impurities and alternative thermo-mechanical treatments might have an influence on the typical Damast pattern. Using nanoindentation measurements, they could analyse specimens of two genuine Damascus sabres. New details of the microstructure (e.g. nanowires of cementite Fe_3C and carbon nanotubes) were revealed by them in their study. Based on these results they speculated that there is a link between

transition metal impurities, hydrocarbons, nanotubes, nanowires and cementite pattern. Furthermore, the presence of cementite nanowires must have consequences for the mechanical properties.

As discussed by Kochmann *et al.* (2004) [9], and shown in **Fig. 3**, the legendary Damascus contains a high density of cementite nanowires and a network of dislocations and this could trigger the nucleation of pearlite. The hardness for cementite and pearlite showed stark changes in the inelastic behaviour of those phases. The indentation in cementite grains were characterized by higher bound Meyer hardness (12 GPa at maximum) and no hysteresis, whereas the indentation on matrix showed lower bound hardness (2.5 GPa) and significant hysteresis resembling a phase transition (**Fig. 3(a)**).

As shown in **Fig. 4**, Ryzewski *et al.* (2011) [1] studied two nail artefacts made of Cu alloy dug from the Great Temple complex of Petra, Jordan to establish how the usage of nanoindentation can have the potential to find properties about archaeological metals. Their study highlighted the value of using other techniques, including nanoindentation, as a means of determining the uncertainties that tend to arise from understandings of single-sited measurements on objects and from single-instrumental analyses during studies of production processes and their performance. They suggested that a higher bound hardness might be caused by strain hardening giving high dislocation densities or by compositional effects that decrease dislocation mobility.

The work of Li *et al.* (2013) [10], shown in **Fig. 5** has two ancient thin-walled bronze vessels unearthed from Anlu County of Hubei Province, China, which were investigated by nanoindentation measurements. The study elucidated and calculated the diffusion of Sn into a Cu specimen based upon high temperature substitutional mechanism. However, nanoindentation measurements show that the hardness of the vessels was 4.85 GPa and 5.24 GPa, respectively (these data were higher than the hardness 2.78 GPa of the simulated as-cast

Cu-24 wt.% Sn alloy). The results suggested that the vessels were probably made-up using the protocol: (1) alloying the high-tin Cu–Sn bronze; (2) casting the shape of the vessels; (3) forging the vessels at appropriate high temperature; (4) wiping tinning on the surface of the vessel at high temperature; (5) quenching the vessels to room temperature; and (6) grinding or polishing the surface of the vessels. They also suggested that the thin-walled bronze vessels provided an indication of the spread of thin-walled high-tin bronze technology in China.

Based on above investigations in metals of archaeological importance, it can be concluded that nanoindentation technique can be used to identify microstructurally age-related modifications. However, further work to estimate other properties of materials can be understood based on improved understanding of the nanoindentation [19], possibly leading to clear differentiation between the respective contributions of manufacture, age and environment. It is also expected that the application of nanoindentation technique to archaeological metal specimens will enable characterization of crystalline phases existing within the alloy (e.g. Ag-Cu alloys, Fe_3C, Cu alloys, bronze, etc, mentioned above) to develop empirical models of materials by incorporating properties of different phases, to obtain further insight into the forming conditions or production processes in the past.

3.2.2 Stones

The zircon stone contains trace levels of the radioactive elements Uranium (U) and Thorium (Th) that over the long period can cause some regions in the specimen to transform from crystalline to amorphous during the radioactive decay process. Oliver and Pharr (2010) [20] investigated a 570 million-year-old zircon stone (a layered structure) found in Sri Lanka (shown in **Fig. 6(a)**) using nanoindentation method, to study the radiation damage involving high-dose and short-term experiments. The sample slice taken was 30 µm thick, with

radioactive trace levels of uranium (U) and thorium (Th) incorporated into the crystal. It was observed that the level of such radioactive elements resulted in a radiation dose very near that required to trigger an amorphization process in such materials. Some of the layers (not cracked ones) were completely amorphous, but the cracked regions were still crystalline. Their suggestion was that the cracks appear because the amorphization process involves about a 17% decrease in density, so its expansion causes the adjacent crystalline material to crack. Oliver and Pharr (2010) [20] were interested in analysing whether the relationship between the long-term radiation dose level and the mechanical properties is the same as they see in short-term, high-dose experiments. **Figure 6(b)** shows electron beam-based microprobe data measuring the Th and U concentrations. They found a good correlation between the mechanical properties of the material and the level of impairment. It can be observed that high doses result in low hardness, and therefore, the amorphous material can have noticeably different properties.

The use-wear on prehistoric stone tools can be used to study human conduct as represented in the archaeological record. To facilitate this, Lerner *et al.* (2007) [12], investigated the nanoindentation behaviour of stone tool raw material to appreciate the development of wear during use. They studied samples of San Juan Fossiliferous Chert (SJF) with a mean hardness of 12.08 GPa, Brushy Basin Chert (BB) with 8.83 GPa, Yellow Silicified Wood (YSW) with 11.02 GPa, and Morrison Undifferentiated Gray Chert (MUG) with 9.08 GPa, all materials from the American Southwest, often found on Archaic sites in the Four Corners area. Material hardness changes in archaeological wear trace regions was used for interpretation.

Current understanding of brittle material accommodation during indentation process indicates that the wear behaviour is influenced by the variation in contact stress fields during indentation cycle (loading, holding, unloading) caused by the microstructural

transformations, changes in the residual stress fields and influence of grain size [19]. Based on above limited investigations in stones related materials, it can be concluded that nanoindentation technique can be used to develop empirical wear models, leading to correlation between the mechanical properties of the material and age-related modifications. It is also expected that indentation technique can be used to quantify the fracture toughness of brittle stone materials, to obtain insight into the fragility of materials, which may assist in planning appropriate preservation or handling of such materials.

3.2.3 Enamels

It has been hypothesized that wear of enamel is sensitive to the presence of sharp particulates in oral fluids and masticated foods, and in the animal kingdom, wear can occur to an extent depending on the food source [49]. Surface observations of worn surfaces can reveal insight into wear micro-mechanisms, but are often obscured by debris and surface smearing, so that interpretations remain controversial [50]. Prediction of wear rates for different tooth forms under certain chewing conditions is of interest to evolutionary biologists. A principal concern is how wear rate is influenced by diet [51]. Therefore, Sanson *et al.* (2007) [13] considered nanoindentation testing of phytoliths, signifying that silica (opal) phytoliths cause dental enamel microwear in sheep mammals. They tested silica phytoliths from four globally widespread species of grass (Poaceae), the pasture grasses Paspalum dilatatum and Setaria viridis (both subfamily Panicoideae, tribe Paniceae), and Phragmites australis and Arundo donax (both subfamily Arundinoideae, tribe Arundineae). The nanohardness results indicates that silica phytoliths (considerably softer) do not contribute as much to mammalian dental (harder) microwear as earlier reported and that exogenous grit and dust are a more likely cause. They also suggested that this premise could

have implications for understandings of the causal agents of microwear phenomena in areas such as the evolution of high-crowned teeth in grazing mammals during the Miocene.

Riede and Wheeler (2009) [14] investigated middle-range link between the Laacher See eruption and Late Glacial fauna and foragers: tephra (or rock fragments ejected during volcanic eruption) as dental abrasive and used nanoindentation to investigate tephra from several sites covering the medial and distal fall-out zones as well as the dental enamel of Homo sapiens and key prey species of Late Glacial foragers. As observed (**Fig. 7**), the Laacher See tephra contained particles twice as hard as even the hardest portions of any of the teeth examined. They suggested that fluoride-induced weakening of dental enamel may have further aggravated tooth wear. Aggravated tooth wear mechanisms may have been the reason of animal mortality, leading to an abandonment of the affected sites.

Apart from above specific examples where nanoindentation has been applied in enamel related archaeometry materials, it is important to note that there is extensive literature, e.g. by Borrero-Lopez *et al.* (2014) [49] and Lawn *et al.* (2012) [51] which addresses general dental wear using the basic mechanics to obtain some generic wear rate of both anthropological and archaeological samples. Their findings suggest that the wear of tooth enamel is representative of wear in brittle solids. Based on the assumption that the wear can be assumed to be time integral of several elasto-plastic micro-asperity events, they discovered the wear rate to be in strong correlation with Archard′s law, which is a model used to describe sliding wear based on the theory of asperity contact [49]. Based on above limited investigations in enamel related materials, it can be concluded that nanoindentation technique can be used to develop empirical wear models, leading to development of mechanical properties correlation.

3.2.4 Claws

Claws reflects the natural history (e.g. feeding habits or locomotion) of mammals and birds. The claw geometry correlates well with arboreal and terrestrial habitats. It is likely that claws microstructure and mechanical properties would change over time, and properties of these types of materials would not always reflect their original functions. Dromaeosaurid theropod claws samples, such as Velociraptor (one of the dinosaur genera, **Fig. 8(a)**), possess strongly recurved, hypertrophied and hyperextensible ungual (or nail) claws on the pes (or foot) (digit II) and manus (or hand). The microstructure of such unguals has been related to the feeding habits or capture and release of the prey. However, the mechanical properties of these structures have not been much explored. In an example, Manning *et al.* (2009) [15] used nanoindentation method while investigating the mechanical properties of the keratin layer and cortical bone of the eagle owl claw (**Fig. 8(b)**). However, it is important to note that reliable indentation properties could not be obtained for such bones due to its highly porosity. Differences in density and microstructure, when coupled with the anisotropic properties of bone (trabecular and cortical) and keratin, leads to a complex structure which is cumbersome to model. In the work by Manning *et al.* (2009) [15], the measured elastic modulus values (6.8±1.5 GPa for keratin layer, 21.1±2.3 GPa for cortical bone, 19 GPa for trabecular bone) were employed for subsequent finite element (FE) model to analyse the compression behaviour of such samples. The FE model confirmed that dromaeosaurid claws could have well-adapted for climbing. However, it was suggested that the strength of the unguals (or nails) was limited with respect to forces acting tangential to the long-axis of claw. It is important to know that greater climbing capabilities of dromaeosaurid dinosaurs supports a scansorial phase in the evolution of flight, however, further research is required to clearly evaluate change in claws microstructure and mechanical properties over time.

3.2.5 Paints

Ancient painting can be partly related with exerting influence upon expressions relied primarily on depiction subjects. Different layers of paint materials can be investigated using nanomechanical testing procedure, primarily for compositional analysis and understanding the aging process. There are very few literatures related to the application of nanoindentation technique to investigate mechanical properties of ancient paints.

In an example on ancient paints, Salvant *et al.* (2011) [16] investigated nanoindentation properties (shown in **Fig. 9**) which can be important for conservation and restoration purpose. One approach was to measure the mechanical properties of reconstructed paints: though, the aging process was poorly known, so it was also desirable to measure micromechanical properties directly on ancient paint specimens. Salvant *et al.* (2011) [16] characterized small specimens recovered from restoration of two Van Gogh paintings and compared the results with reconstructed paint samples, where it was demonstrated that the reduced elastic modulus and hardness of such paints can be measured at a very local scale (potentially differentiating between each paint layer). The reconstructed paint specimens exhibit elastic moduli comparable to literature values, but the measured values on the two 19^{th} century paint specimens were found to be larger. Similarly, the compositional dependence of the elastic modulus was found to be consistent with literature results for reconstructed specimens while the preliminary results for ancient specimens do not fall into the similar form. It is important to note that these analyses point to a significant impact of long term aging. In this context, Salvant *et al.* (2011) [16] concluded that nanoindentation measurement could offer an opportunity of investigating the influence of various parameters on a large range of naturally aged specimens for better understanding of the mechanical behaviour of oil paints and their aging.

Some appropriate information related to measurement (e.g. as summarised in *Section 2* above) provided by nanoindentation measurement could also offer the opportunity to

categorise materials similar in reduced modulus and hardness to the original paint material if paint loss should be restored. For example, in modern paints, it has been demonstrated that the relationship between crosslink density in paint matrix and mechanical (ductility) properties can be correlated to scratch resistance [52]. However, such correlation can be difficult to establish in pigmented paint coatings as dislodgement of pigments during scratch tests can lead to accelerated wear. Therefore, localised nanoindentation testing can yield information on paint properties without causing the dislodgement of pigments, however, time dependent indentation response (creep), leading to steeper and even negative unloading slopes and hence inaccurate mechanical properties [53].

3.2.6 Bones

Bone is a heterogeneous material containing three main phases: mineral, collagen, and water, arranged in a series of hierarchical structures [40]. Collagen contributes to bone's elastic and viscoelastic behavior while mineral stiffens the overall material, whereas, water contribute to elasticity and ductility. In modern times, scientific study of structure of bones is called as Osteology. Various factors such as age, death, sex, growth and development can be analysed with the identification of bone or its remains. Nanoindentation technique can be applied on bone skeletal remains to investigate mechanical properties to reconstruct the past, understand human variation, and provide information about the deceased individuals, or potentially identifying some pathological (study of disease) conditions.

As summarised by Olesiak *et al.* (2006) [17] and Olesiak *et al.* (2010) [18], bone is a tissue that endures development and remodelling through bio-mineralization during its lifetime. This remodelling is governed by the Wolff's law [54]. In natural bones, the tensile and compressive strength varies in the longitudinal and transverse directions e.g. tensile strength varies between 54 MPa to 166 MPa, whereas, compressive strength varies between

106 MPa to 204 MPa in the longitudinal direction [55]. It is even conceivable to measure direction dependent properties of structures using the nanoindentation method [55-56]. Although a general clinical practice is to perform the dual energy X-ray absorptiometry (DEXA) scan to measure the bone mineral density (BMD), changes in bone structures with age for both male and female can also be quantified using nanoindentation system [57]. However, in archaeometry the emphasis is to recover sample history details from the nanoindentation data which makes it more challenging. Following an organism's demise, diagenesis occurs in bone at range of length scales, including post-mortem and biological alterations. A consideration of sample protection and tissue-level diagenetic alteration is vital to palaeontologists and archaeologists, and nanoindentation combined with complimentary techniques mentioned above can be used to investigate the functional significance of a wide range of archaeological materials even after fossilization. It has been suggested that nanomechanical analysis of bone at the tissue level reveals a conclusive relationship between physical properties and the local organic content, mineral content, and microstructural arrangement [17-18]. However, it was not clear as to how these properties changes post fossilization, or diagenesis, where the organic phase was swiftly removed, and the residual mineral phase was reinforced by the deposition of apatites, calcites, and other minerals. As shown in **Figs. 10(a,b,c)**, Olesiak *et al.* (2006) [17] and Olesiak *et al.* (2010) [18] employed nanoindentation to investigate the nanomechanical properties of fossilized and modern bone samples with the goal of providing insights into the complex processes of diagenesis.

Nanoindentation performed by Olesiak *et al.* (2006) [17] in both longitudinal and transverse directions revealed preservation of bones natural anisotropy as transverse modulus values were consistently smaller than longitudinal values. Additionally, the modulus values of fossilized bone from 35 GPa to 89 GPa increased linearly with logarithm of the samples age. As shown in **Fig. 10(d)**, nanoindentation discovered that the basic mechanical anisotropy

of modern bone (Olesiak *et al.*, 2010) [18] can be preserved in fossil bones going back to the early Eocene (~50 Ma, where Ma is million years ago), as the elastic modulus values measured perpendicular to the long axis of each bone sample were lower than longitudinal values (as is the case for modern bones). While an increase in mechanical properties was observed by Olesiak *et al.* (2010) [18], with the geological age of the samples, a relatively small increase was seen in fossil bone specimens older than the Miocene, signifying that mineral infilling is limited by spatial saturation. An increased crystallinity and density correlated with an increase in elastic modulus, which shows a link between the crystal microstructure and the mechanical properties of samples.

3.2.7 Skins

Skin is the soft part of outer tissue which has three layers (epidermis, dermis and hypodermis), which protects us from microbes, helps regulate body temperature and permits the sensations of touch, heat and cold. The mechanical properties of skin are an important characteristic of its resistance to damage and important indicators of pathological situations [46]. There are very few literatures related to application of nanoindentation technique to investigate mechanical properties of ancient mummified skins (e.g. **Fig. 1**).

Influence of external factors or the action of micro-organisms, however, can damage the tissue and lay the subjacent tissue open. To estimate the degree of tissue protection in mummified human skin and, the reason for its resilience or durability, Janko *et al.* (2010) [6] examined the structural integrity of type I collagen (i.e. protein). Janko *et al.* (2010) [6] mined samples from the Neolithic glacier mummy known as 'the Iceman'. When reference samples analysed from a volunteer of a similar biological age as the Iceman, microscopy using AFM exposed collagen fibrils that had characteristic banding patterns of 69±5 nm periodicity, i.e. sheet-like structures, and it is also characteristic for modern skin collagen [6].

It was observed that microstructure of dermal collagen bundles and fibrils were largely unaltered and very well conserved by the natural conservation process. Raman spectra of the ancient collagen showed that there were no substantial alterations in the molecular structure. However, AFM based nanoindentation tests showed some changes in the mechanical behaviour of the fibrils. Elastic modulus of single mummified fibrils was 4.1±1.1 GPa, whereas, the elasticity of recent collagen averages 3.2±1 GPa. The preservation of the collagen after 5300 years indicated that dehydration owing to freeze-drying of the collagen is the main process in mummification and that the effect of the degradation can be potentially addressed. It is important to note that temperature variations, ultraviolet irradiation and the actions of insects, bacteria and fungi can potentially cause degradation, causing further skin tissue decay [6]. Based on above limited investigations in mummified skin, it can be concluded that nanoindentation technique using elastic modulus values can be used to develop correlation between the mechanical properties of the mummified fibrils and age-related modifications, i.e. it resilience or durability.

4. CONCLUDING REMAKRS

This review argues that archaeology could substantially benefit from the use of the minimally-invasive nanoindentation techniques (as demonstrated in **Fig. 11**). The technique can help identify the material composition of artefacts, shed light into their construction, and characterize the mechanical properties of ancient tissues and biological constituents [58]. This can allow inference of, *inter alia*, local customs, range of habitation, trade patterns, and advancement of technology and development.

Bone, including dental material, is also an area where nanomechanical characterization techniques are frequently used, mostly on modern materials, but occasionally on ancient or fossilized artefacts. Abrasions as well as wear and stress patterns can provide

useful information to the archaeologist, informing theories on human migration and habitation patterns [14]. Analysis of dinosaur claws can provide insight into strength and therefore postulate the way the claws were used and thus shed light on the habits of the dinosaur [15]. As bone and teeth are formed by minerals, local conditions will dictate the composition of the material and thus allow for a correlation between the sample, its origin, and its location [18]. Further, when applied to fossilised material, the results of the analysis can help identify the age of the material [17].

The nano-scratch technique was also used on modern and ancient steel to establish values of nanohardness and elasticity [8]. The scratch testing is of importance to access the fracture data of the unique range of exotic materials described above. These testing methods are also useful to access the values of friction coefficient which are now aiding to device the bio-inspired strategy to combat catastrophic damages [59]. Additionally, another example of understanding the bio-inspired designs (BID) can be seen in a range of studies varying from designing cutting tools for machining [60], transportation solutions [61], nanotechnology and so on [62]. By analysing the materials in bronze vessels to determine regional variations and shed light on the composition of the alloy and of the specific forging techniques used, information is obtained on the origin and spread of the technology [10] and of human migration and trade patterns. Indeed, the results of the analysis are crucial to understanding the relationship between environment and adaptation and evolution [63].

Potentially, the instrumented indentation technique can be used to quantify the residual stresses of materials [19, 64], which is known to affect fatigue strength, fracture toughness and wear resistance, and which can influence the structural strength and lifetime of archaeological components. This review concludes that many investigations above scrutinise the basic nanomechanical properties (hardness, elastic modulus, fracture) during nanoindentation, and therefore, there is a scope for residual stress measurement with proper

calibration of archaeological test specimens, which may help in planning preservation strategies. Recently, Marshall *et al.* [65] have addressed a general perception in this field questioning the validity of the indentation results. Their review provides useful guidelines on what may go wrong during such a test whilst also highlighting that the indentation fracture theory is fundamental and originated from the theory of fracture mechanics proposed earlier by Griffith. Darvell *et al.* [66] proposed mechanical properties measurement of pliant solids, particularly toughness using either scissors or wedge tests, which can potentially be fully instrumented for enhanced fracture or toughness measurement of biomaterials. It is asserted by the numerous results that besides few orders of numerical uncertainty the modern nanoindentation technique is rather a very quick, site-specific convenient and economical means for comparative mechanical characterization of any material sample. As an outlook, we anticipate a growing capability of mechanical parameters as measured by nanoindentation to be interpreted in terms of not only usage but also ageing states of various materials. This could be through specific radiation damage mechanisms as discussed in the review but may eventually encompass precision measurement of parameters affected by physical ageing of non-equilibrium phases.

Aging is a time-dependent process [67] and one of the important aspects in archaeometry. Aging (in the current context, for example, due to low or high temperature exposure, mechanical loading, radiation exposure, actions of insects, bacteria and fungi, tribological wear, etc.) can be explained as partial or total loss of their capacity to achieve the purpose, can lead to change in structural properties, and may impact the ability to withstand various challenges from operation, environment and natural events [67]. Except few examples, such as ultraviolet irradiation and the actions of insects, bacteria and fungi related degradation in skin [6], age-related variations at grain boundaries in metals [7], tribological wear of enamels [13-14], mechanical (ductility) properties for paint like materials [16],

radiation related damage in stones [20], aging related characterization of archaeological materials using nanoindentation technique has not been demonstrated much through literature. Since aging of materials over time may induce damage or microstructural changes (leading to changes in hardness, modulus, fracture toughness, wear resistance, etc.), investigation of aging can provide further reliability on the application of nanoindentation technique.

For over many years, nanoindentation technique has been used to characterize variety of materials. Literature discussed here address issues that are becoming of increasing interest to researchers in the field of archaeological materials. Now it is easy to foresee that inspection of archaeological materials using nanoindentation technique is important for number of reasons, as it can provide valuable information about mechanical properties which, in turn, relate to the evolution of ancient biomaterials as well as human history and production methods. However, the value of nanoindentation interpretations of archaeological materials would benefit from a detailed comparative study using other validation techniques. This is an area which can provide further reliability on the application of nanoindentation technique. It also requires further investigation to bring out improvements to make this technique more satisfactory, as many interpretation issues in nanoindentation tests such as anomalies between loading-holding-unloading stages and occurrence of deformation and/or cracking are still unresolved. However, the trends reported in this review on the application of nanoindentation technique of archaeological materials show potential for its wider applications at world heritage sites. Also, a simpler user interface could also serve to build a strong case for how nanoindentation instrument could be useful as a routine tool to evaluate ancient materials properties.

ACKNOWLEDGMENT

Authors (SG and GC) would like to acknowledge the funding in the form of 'Short Term Scientific Mission' from the COST Action MP1303 as well as COST Action 15102 of the Horizon 2020. The authors are particularly grateful to the Principal Editor (Journal of Materials Research) and the reviewers for their extensive comments and recommendations.

REFERENCES

1. K. Ryzewski, B. W. Sheldon, S. E. Alcock, M. Mankin, S. Vasudevan, and N. Sinnott-Armstrong: Multiple assessments of local properties, production, and performance in metal objects: an experimental case study from Petra, Jordan. *Archaeol. Anthropol. Sci.* **3**, 173 (2011).
2. ISO 14577-1, -2, -3, -4 Metallic Materials Instrumented Indentation Tests for Hardness and Material Properties Available from American National Standards Institute (ANSI), 25 W. 43rd St., 4th Floor, New York, NY 10036.
3. ASTM E2546-07, Standard Practice for Instrumented Indentation Testing, ASTM International, West Conshohocken, PA, 2007, www.astm.org
4. W. C. Oliver and G. M. Pharr: An improved technique for determining hardness and elastic modulus using load and displacement sensing indentation experiments. *J. Mater. Sci.* **7**, 1564 (1992).
5. G. M. Erickson, B. A. Krick, M. Hamilton, G. R. Bourne, M. A. Norell, E. Lilleodden, and W. G. Sawyer: Complex dental structure and wear biomechanics in hadrosaurid dinosaurs. *Science* **338**, 98 (2012).

6. M. Janko, A. Zink, A. M. Gigler, W. M. Heckl, and R. W. Stark: Nanostructure and mechanics of mummified type I collagen from the 5300-year-old Tyrolean Iceman. *Proc. R. Soc. B.* **277**, 2301 (2010).

7. P. Northover, S. Northover, and A. Wilson: Microstructures of ancient and historic silver. In: *Metal* 2013, 16-20 September 2013, Edinburgh, International Council of Museums ICOM-CC, 253 (2013).

8. N. Patzke, A. A. Levin, I. P. Shakhverdova, M. Reibold, W. Kochmann, P. Paufler, and D. C. Meyer: Nanostructured Ancient Damascus Blades, DMG 2008 (abstract no. 208, session S17).

9. W. Kochmann, M. Reibold, R. Goldberg, W. Hauffe, A. A. Levin, D. C. Eyer, T. Stephan, H. Müller, A. Belger, and P. Paufler: Nanowires in ancient Damascus steel. *J. Alloys Compd.* **372**, L15-L19 (2004)

10. Y. Li, T. Wu, L. Liao, C. Liao, L. Zhang, G. Chen, and C. Pan: Techniques employed in making ancient thin-walled bronze vessels unearthed in Hubei Province, China. *Appl. Phys. A: Mater. Sci. Process.* **111**, 913 (2013).

11. B. C. Chakoumakos, W. C. Oliver, G. R. Lumpkin, and R. C. Ewing: Hardness and elastic modulus of zircon as a function of heavy-particle irradiation dose: I. In situ α-decay event damage. *Radiat. Eff. Defects Solids*. **118**, 393 (1991).

12. H. Lerner, X. Du, A. Costopoulos, and M. Ostoja-Starzewski: Lithic raw material physical properties and use-wear accrual. *J. Archaeol. Sci.* **34**, 711 (2007).

13. G. D. Sanson, S. A. Kerr, and K. A. Gross: Do silica phytoliths really wear mammalian teeth? *J. Archaeol. Sci.* **34**, 526 (2007).

14. F. Riede and J. M. Wheeler: Testing the 'Laacher See hypothesis': tephra as dental abrasive. *J. Archaeol. Sci.* **36**, 2384 (2009).

15. P. L. Manning, L. Margetts, M. R. Johnson, P. J. Withers, W. I. Sellers, P. L. Falkingham, P. M. Mummery, P. M. Barrett, and D. R. Raymont: Biomechanics of Dromaeosaurid Dinosaur Claws: Application of X-ray microtomography, nanoindentation and finite element analysis. *The Anatomical Record.* **292**, 1397 (2009).

16. J. Salvant, E. Barthel, and M. Menu: Nanoindentation and the micromechanics of Van Gogh oil paints. *Appl. Phys. A: Mater. Sci. Process.* **104**, 509 (2011).

17. S. E. Olesiak, M. L. Oyen, M. Sponheimer, J. J. Eberle, and V. L. Ferguson: Ultrastructural mechanical and material characterization of fossilized bone. *Mater. Res. Soc. Symp. Proc.* **975**, 0975-DD03-09 (2006).

18. S. E. Olesiak, M. Sponheimer, J. J. Eberle, M. L. Oyen, and V. L. Ferguson: Nanomechanical properties of modern and fossil bone. *Palaeogeogr., Palaeoclimatol., Palaeoecol.* **289**, 25 (2010).

19. N. H. Faisal, R. Ahmed, and R. L. Reuben: Indentation testing and its acoustic emission response: Applications and emerging trends. *Int. Mater. Rev.* **56**, 98 (2011).

20. W. C. Oliver and G. M. Pharr: Nanoindentation in materials research; past, present, and future. *MRS Bull.* **35**, 897 (2010).

21. D. Tabor: in *The hardness of metals,* (Oxford Clarendon Press, Oxford, England, 1951), pp. 19-43.

22. N. K. Mukhopadhyay and P. Paufler: Micro- and nanoindentation techniques for mechanical characterisation of materials. *Int. Mater. Rev.* **51**, 209 (2006).

23. M. R. VanLandingham: Review of instrumented indentation. *J. Res. Natl. Inst. Stand. Technol.* **108**, 249 (2003).

24. A. C. Fisher-Cripps: *Nanoindentation*, (Springer, New York, 2002), pp. 39.

25. R. Hill: in *The mathematical theory of plasticity*, (Oxford Clarendon Press, Oxford, England, 1950), pp. 14.

26. B. R. Lawn and R. Wilshaw: Review-Indentation fracture: principles and applications. *J. Mater. Sci.* **10**, 1049 (1975).

27. B. R. Lawn and D. B. Marshall: Hardness, toughness, and brittleness: an indentation analysis. *J. Am. Ceram. Soc.* **62**, 347 (1979).

28. M. L. Oyen: Analytical Techniques for Indentation of Viscoelastic Materials. *Philos. Mag*. **86**, 5625 (2006).

29. J. B. Pethicai, R. Hutchings, and W. C. Oliver: Hardness measurement at penetration depths as small as 20 nm. *Philos. Mag. A* **48**, 593 (1983).

30. R. J. Ellis: Verification of hardness tester indenter force 10 gf to 10 kgf (0.0981 N to 98.1 N). *J. Phys. E: Sci. Instrum.* 3, 565 (1970).

31. A. C. Fischer-Cripps: *Nanoindentation*. 2nd ed. (Springer-Verlag, New York, 2002), pp. 39.

32. S. Suresh and A. Giannakopoulos: A new method for estimating residual stresses by instrumented sharp indentation. *Acta Mater*. **46**, 5755 (1998).

33. W. C. Oliver and G. M. Pharr: Measurement of hardness and elastic modulus by instrumented indentation: Advances in understanding and refinements to methodology. *J. Mater. Res.* **19**, 1 (2004).

34. A. C. Fischer-Cripps: *Introduction to Contact Mechanics*. 2nd ed. (Springer, US, 2007), pp. 77, 175.

35. K. L. Johnson: *Contact mechanics*. (Cambridge University Press, England, 1985), pp. 84.

36. I. N. Sneddon: The relation between load and penetration in the axisymmetric Boussinesq problem for a punch of arbitrary profile. *Int. J. Eng. Sci.* **3**, 47 (1965).

37. G. M. Pharr, J. H. Strader, and W. C. Oliver: Critical issues in making small-depth mechanical property measurements by nanoindentation with continuous stiffness measurement. *J. Mater. Res.* **24**, 653 (2009).

38. NanoBlitz 4D; http://nanomechanicsinc.com/available-now-nanoblitz-3d-4d/ (5 September 2017).

39. O. Jiroušek: in *Nanoindentation in Materials Science* (InTech, 2012), pp. 259.

40. A. J. Bushby, V. L. Ferguson, and A. Boyde: Nanoindentation of bone: Comparison of specimens tested in liquid and embedded in polymethylmethacrylate. *J. Mater. Res.* **19(1)**, 249 (2004).

41. M. Granke, A. Coulmier, S. Uppuganti, J. A. Gaddy, M. D. Does, and J. S. Nyman: Insights into reference point indentation involving human cortical bone: sensitivity to tissue anisotropy and mechanical behavior. *J. Mech. Behav. Biomed. Mater*. **37**, 174 (2014).

42. A. K. Bembey, M. L. Oyen, A. J. Bushby, and A. Boyde: Viscoelastic properties of bone as a function of hydration state determined by nanoindentation. *Philos. Mag*. **86**, 5691 (2006).

43. R. K. Nalla, M. Balooch, J. W. AgerIII, J. J. Kruzic, J. H. Kinney, and R. O. Ritchie: Effects of polar solvents on the fracture resistance of dentin: role of water hydration. *Acta Biomaterialia*. **1(1)**, 31 (2005).

44. L. Angker, M. V. Swain: Nanoindentation: application to dental hard tissue investigations. *J. Mater. Res.* **21(8)**, 1893 (2006).

45. M. Dudíková, D. Kytýr, T. Doktor, and O. Jiroušek: Monitoring of material surface polishing procedure using confocal microscope. *Chem. Listy*. **105**, 790 (2011).

46. B. Bhushan and W. Tang: Nanomechanical characterization of skin and skin cream. *J. Microsc.* 240, 135 (2010).

47. M. L. Crichton, X. Chen, H. Huang, M. A. F. Kendall: Elastic modulus and viscoelastic properties of full thickness skin characterised at micro scales. *Biomaterials*. **34(8)**, 2087 (2013).

48. M. Reibold, P. Paufler, A. A. Levin, W. Kochmann, N. Pätzke, and D. C. Meyer: Materials: Carbon nanotubes in an ancient Damascus sabre. *Nature* **444**, 286 (2006).

49. O. Borrero-Lopez, A. Pajares, P. J. Constantino, and B. R. Lawn: A model for predicting wear rates in tooth enamel. *J. Mech. Behav. Biomed. Mater.* 37, 226 (2014).

50. P. Ungar and M. Sponheimer: The diets of early hominins. *Science*. **334**, 190 (2011).

51. B. R. Lawn, R. F. Cook: Probing material properties with sharp indenters: a retrospective. *J. Mater. Sci.* **47**, 1 (2012).

52. J. Lange, A. Luisier, E. Schedin, G. Ekstrand, and A. Hult; Development of scratch tests for pre-painted metal sheet and the influence of paint properties on the scratch resistance. *J. Materials Processing Tech.* **86**, 300 (1999).

53. Wai, Siu Wah, Rapid assessment of paint coatings by micro and nano indentation methods, Doctor of Philosophy thesis, School of Mechanical, Materials and Mechatronic Engineering, University of Wollongong, 2013. http://ro.uow.edu.au/theses/3873

54. R. A. Brand: Biographical Sketch: Julius Wolff, 1836–1902. *Clin. Orthop. Relat. Res.* **468**, 1047 (2010).

55. U. Wolfram and J. Schwiedrzik: Post-yield and failure properties of cortical bone *BoneKEy Rep*. 5, 829 (2016).

56. J. Schwiedrzik, R. Raghavan, A. Bürki, V. LeNader, U. Wolfram, J. Michler, and P. Zysset: *In situ* micropillar compression reveals superior strength and ductility but an absence of damage in lamellar bone. *Nat. Mater*. **13**, 740 (2014).

57. M. J. Mirzaali, J. J. Schwiedrzik, S. Thaiwichai, J. P. Best, J. Michler, P. K. Zysset, and U. Wolfram: Mechanical properties of cortical bone and their relationships with age, gender, composition and microindentation properties in the elderly. *Bone*. **93**, 196 (2016).

58. K. S. Anseth, C. N. Bowman, and L. Brannon-Peppas: Mechanical properties of hydrogels and their experimental determination. *Biomaterials*. **17**, 1647 (1996).

59. H. Yao, Z. Xie, C. He, and M. Dao: Fracture mode control: a bio-inspired strategy to combat catastrophic damage. *Sci. Rep.* **5**, 8011 (2015).

60. A. Fatima and P. T. Mativenga: On the comparative cutting performance of nature-inspired structured cutting tool in dry cutting of AISI/SAE 4140. *Proc. Inst. Mech. Eng., Part B. DOI:* 10.1177/0954405415617930 (2015).

61. Four Student-Designed, Nature-Inspired Transportation Solutions, http://makezine.com/2014/06/10/four-student-designed-nature-inspired-transporation-solutions/ (20 August 2017).

62. Research showcase on bioinspired design, http://www3.imperial.ac.uk/newsandeventspggrp/imperialcollege/engineering/newssummary/news_2-2-2016-16-28-13 (20 August 2017).

63. P. S. Ungar: Dental evidence for the diests of Plio-Pleistocene hominis. *Am. J. Phys. Anthropol.* **146**, 47 (2011).

64. N. H. Faisal and R. Ahmed: A review of patented methodologies in instrumented indentation residual stress measurements. *Recent Pat. Mech. Eng.* **4(2)**, 138 (2011).

65. D. B. Marshall, R. F. Cook, N. P. Padture, M. L. Oyen, A. Pajares, J. E. Bradby, I. E. Reimanis, R. Tandon, T. F. Page, G. M. Pharr, and B. R. Lawn: The compelling case for indentation as a functional exploratory and characterization tool. *J. Am. Ceram. Soc.* **98(9)**, 2671 (2015).

66. B. W. Darvell, P. K. D. Lee, T. D. B. Yuen, and P. W. Lucas: A portable fracture toughness tester for biological materials. Meas. Sci. Technol. 7(6), 954 (1996).

67. S. Valliappan and C. K. Chee: Aging degradation of mechanical structures. *J. Mech. Mater. Struc.* **3(10)**, 1923 (2008).

Figure Captions

Fig. 1. The Neolithic glacier mummy, the Iceman [reprinted with permission from ref. 6, an open access article which permits unrestricted use, Publisher: Royal Society Publishing].

Fig. 2. (a) Nanoindentation in Sterling silver homogenised for 2 hours at 760 °C, then annealed for 1 hour at 350 °C, and (b) hardness values for transformed and untransformed regions of homogenised and annealed Sterling silver [reprinted with authors permission from ref. 7] (Color figures online only).

Fig. 3. Nanoindentation of cementite and pearlite (Damascus steel): (a) loading *P-h* curves for cementite and pearlite, (b) hardness and reduced elastic modulus plotted versus the penetration depth, showing indentation size effect, (c) microstructure of a 17^{th} century Damascus sabre shows large cementite grains embedded in a fine grained pearlitic matrix and voids, and (d) detection of nanowires in Damascus steel, where the dark stripes indicate nanowires [reprinted with permission from ref. 9, Publisher: Elsevier].

Fig. 4. Nail artefacts made of Cu alloy excavated from the Great Temple complex of Petra (in Jordan): (a, b) Nail 1 and 2, where cross-section locations are encircled, and (c) summary of the hardness and reduced modulus along the length of nail 2 [reprinted with permission from ref. 1, Publisher: Springer Nature] (Color figures online only).

Fig. 5. Thin walled bronze vessels unearthed in Anlu County of Hubei Province (China): (I) optical microstructures of the sample ABY5011-1, where (a) cross-section; (b) longitudinal section, (II) optical microstructures of the sample ABY5011-2, where (c) Cross-section; (d) longitudinal section, and (III) *P-h* curves of different zones in the sample ABY5011-1 and simulated as-cast Cu-24 wt.% Sn sample [reprinted with permission from ref. 10, Publisher: Springer Nature] (Color figures online only).

Fig. 6. Nanoindentation studies of a 570 million-year-old zircon stone found in Sri Lanka: (a) a photomicrograph of the layered structure of the stone, and (b) plot of hardness and alpha

particle radioactive decay dose as a function of position across the layers outlined by the white box in the photomicrograph [reprinted with permission from ref. 20, Publisher: Cambridge University Press] (Color figures online only).

Fig. 7. Nanoindentation on enamels: (a) (i) optical micrograph of buccal-to-lingual cross-section of M2 from Cervus elaphus with indents visible, and (ii) nanoindentation results for the cross-section as a function of distance from the buccal edge, (b) hardness values for different areas within the molars from different species, (c) hardness of top 20% of tephra particles for each sample group [reprinted with permission from ref. 14] (Color figures online only).

Fig. 8. Dromaeosaurid theropod dinosaur sample: (a) the 'fighting pair' Velociraptor and Protoceratops, and (b) high-resolution X-ray CT of owl terminal ungual phalanx and pedal claw (bone core and keratin sheath), where bone is white, keratin, and soft-tissue are grey [reprinted with permission from ref. 15, Publisher: John Wiley and Sons].

Fig. 9. (a) Optical microscope image of sample Van Gogh paintings (sample: VG2) after nanoindentation measurements, and (b) reduced elastic modulus as a function of penetration for ten measurements on sample VG2 [reprinted with permission from ref. 16, Publisher: Springer Nature] (Color figures online only).

Fig. 10. Nanoindentation of fossilized and modern bone: (a) longitudinal axis 6x6 indent array over osteonal and interstitial bone, 15 Ma (million years ago) sample, (b) transverse axis 4x9 indent array starting at Haversian canal, 15 Ma sample, (c) cortical bone indents: longitudinal vs. transverse [reprinted with permission from ref. 17, Publisher: Cambridge University Press], and (d) longitudinal modulus values vs. the log of geological age (there is a clear increase of modulus values with the geologic age of the sample) [reprinted with permission from ref. 18, Publisher: Elsevier] (Color figures online only).

Fig. 11. Use of the minimally-invasive nanoindentation technique in archaeometry (Color figures online only).

Figures

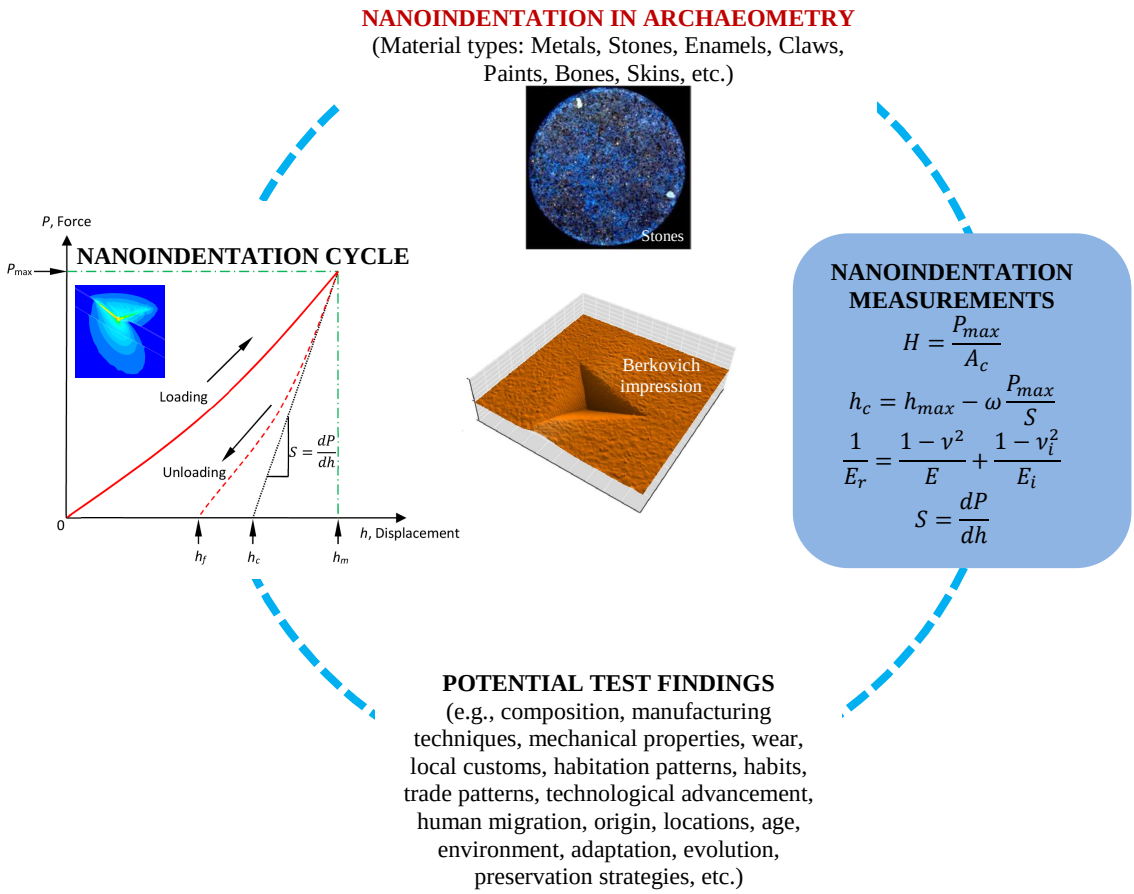

Graphical abstract

Fig. 11. Use of the minimally-invasive nanoindentation technique in archaeometry.

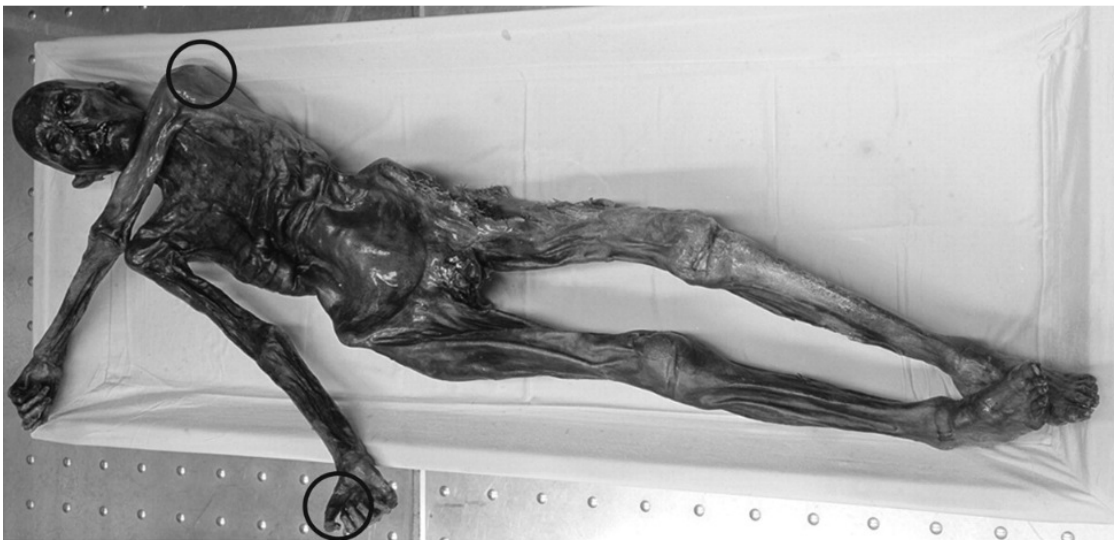

Fig. 1. The Neolithic glacier mummy, the Iceman [reprinted with permission from ref. 6].

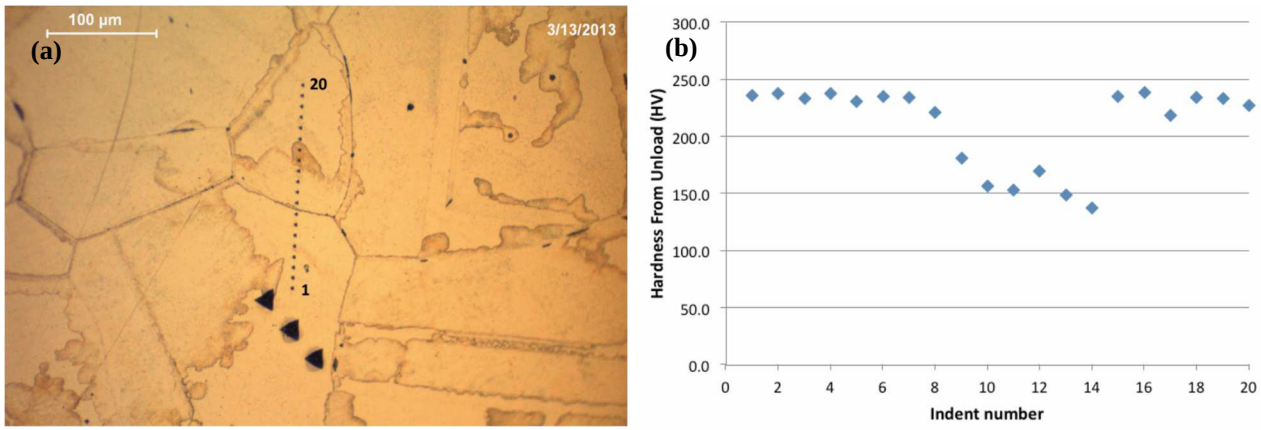

Fig. 2. (a) Nanoindentation in Sterling silver homogenised for 2 hours at 760 °C, then annealed for 1 hour at 350 °C, and (b) hardness values for transformed and untransformed regions of homogenised and annealed Sterling silver [reprinted with permission from ref. 7] (Color figures online only).

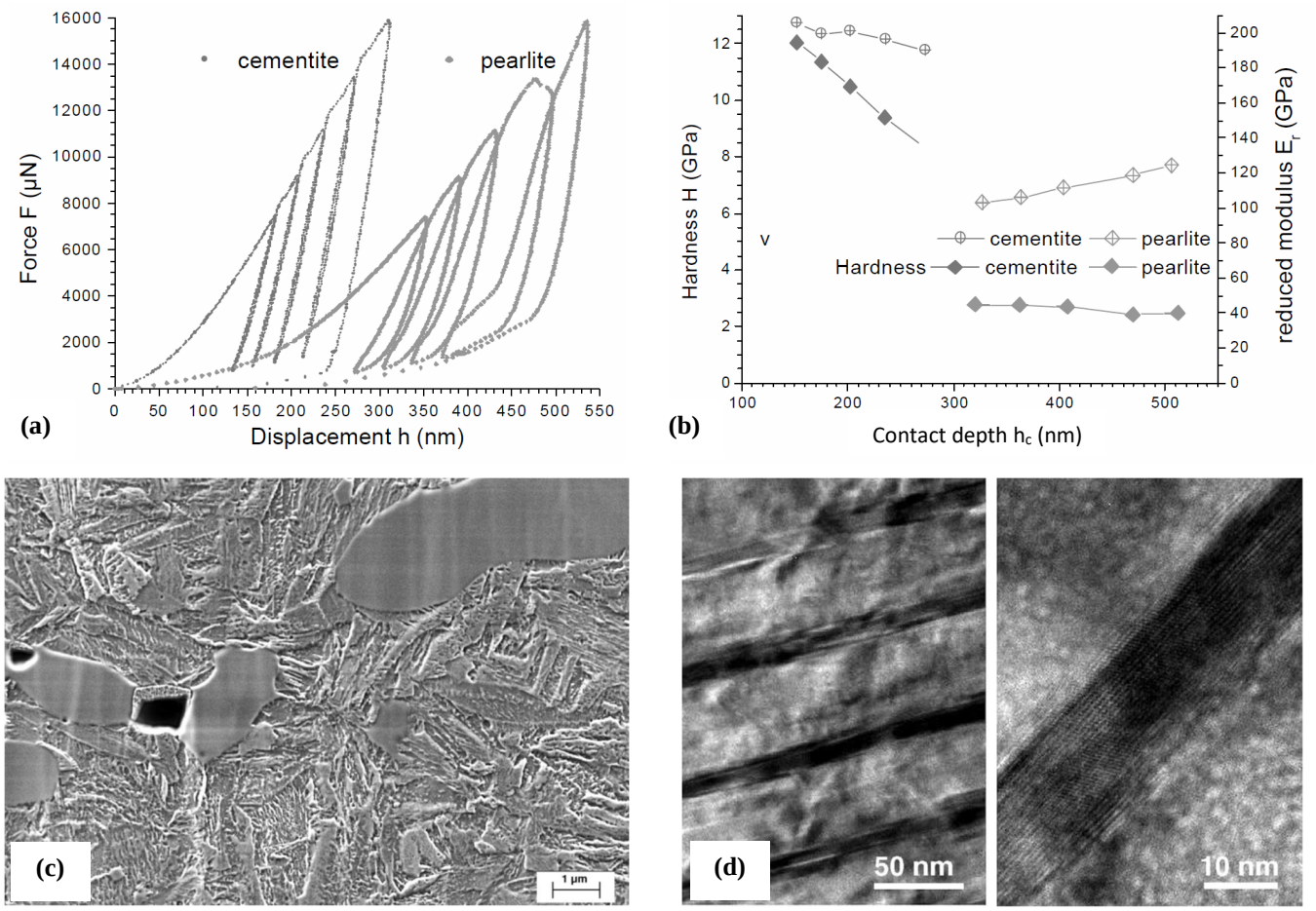

Fig. 3. Nanoindentation of cementite and pearlite (Damascus steel): (a) loading *P-h* curves for cementite and pearlite, (b) hardness and reduced elastic modulus plotted versus the penetration depth, showing indentation size effect, (c) microstructure of a 17th century Damascus sabre shows large cementite grains embedded in a fine grained pearlitic matrix and voids, and (d) detection of nanowires in Damascus steel, where the dark stripes indicate nanowires [reprinted with permission from ref. 9].

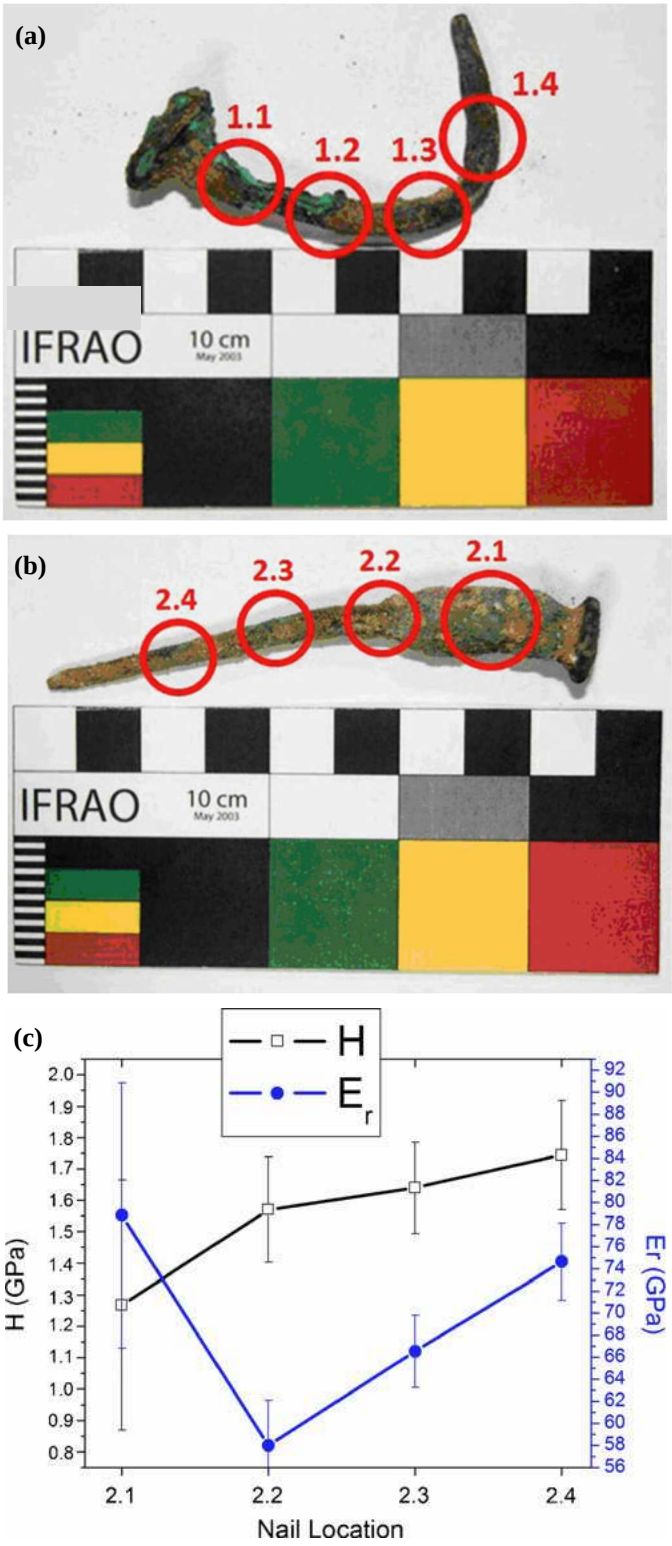

Fig. 4. Nail artefacts made of Cu alloy excavated from the Great Temple complex of Petra (in Jordan): (a, b) Nail 1 and 2, where cross-section locations are encircled, and (c) summary of the hardness and reduced modulus along the length of nail 2 [reprinted with permission from ref. 1] (Color figures online only).

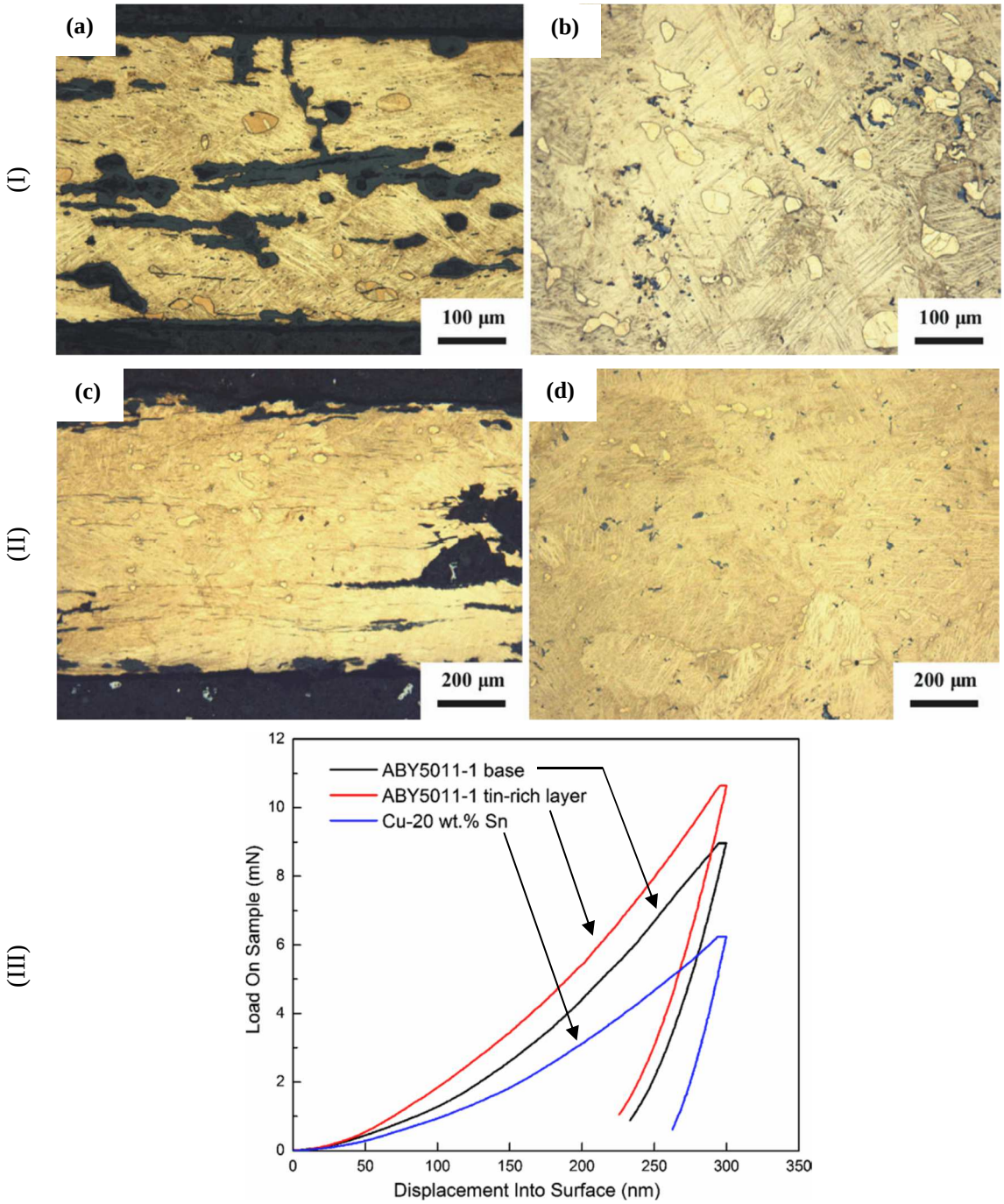

Fig. 5. Thin walled bronze vessels unearthed in Anlu County of Hubei Province (China): (I) optical microstructures of the sample ABY5011-1, where (a) cross-section; (b) longitudinal section, (II) optical microstructures of the sample ABY5011-2, where (c) Cross-section; (d) longitudinal section, and (III) *P-h* curves of different zones in the sample ABY5011-1 and simulated as-cast Cu-24 wt.% Sn sample [reprinted with permission from ref. 10] (Color figures online only).

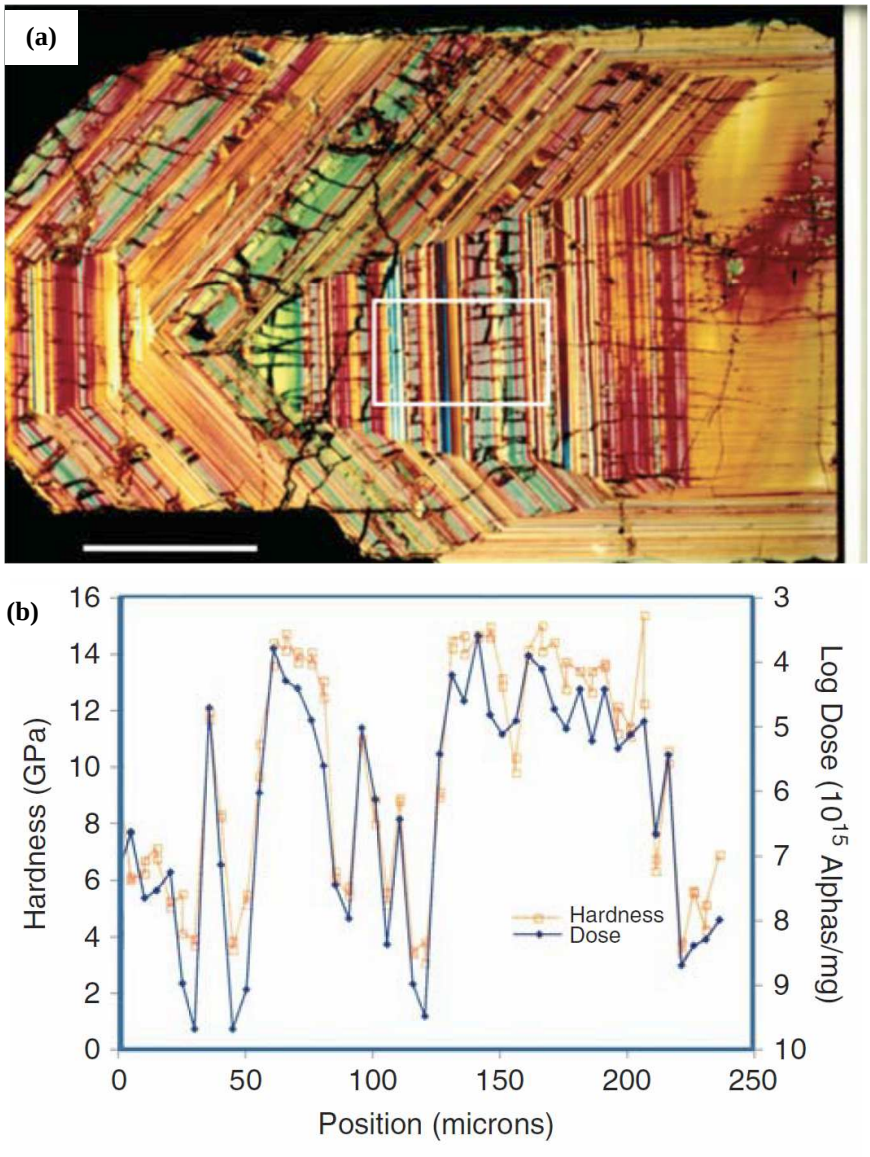

Fig. 6. Nanoindentation studies of a 570 million-year-old zircon stone found in Sri Lanka: (a) a photomicrograph of the layered structure of the stone, and (b) plot of hardness and alpha particle radioactive decay dose as a function of position across the layers outlined by the white box in the photomicrograph [reprinted with permission from ref. 20] (Color figures online only).

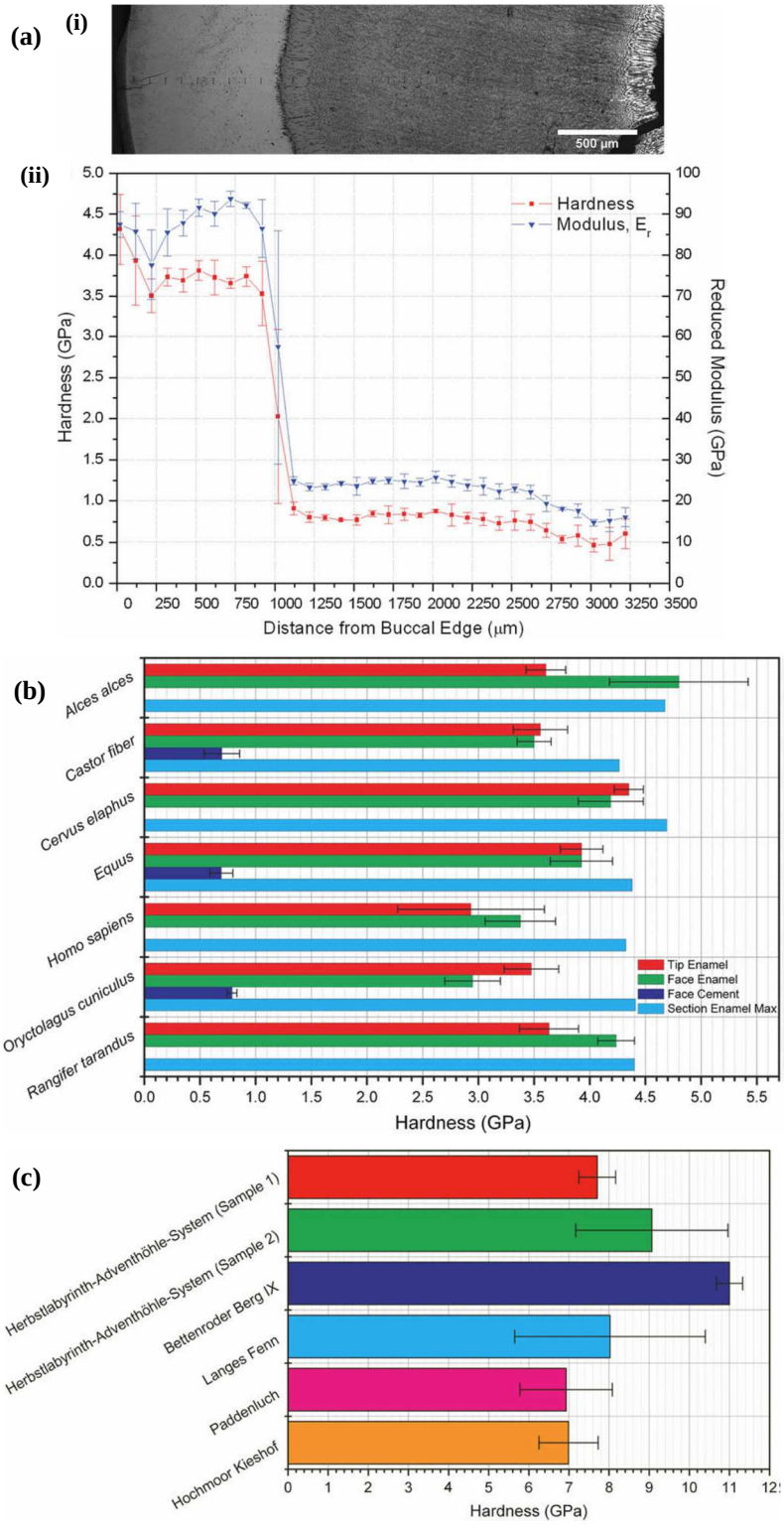

Fig. 7. Nanoindentation on enamels: (a) (i) optical micrograph of buccal-to-lingual cross-section of M2 from Cervus elaphus with indents visible, and (ii) nanoindentation results for the cross-section as a function of distance from the buccal edge, (b) hardness values for different areas within the molars from different species, (c) hardness of top 20% of tephra particles for each sample group [reprinted with permission from ref. 14] (Color figures online only).

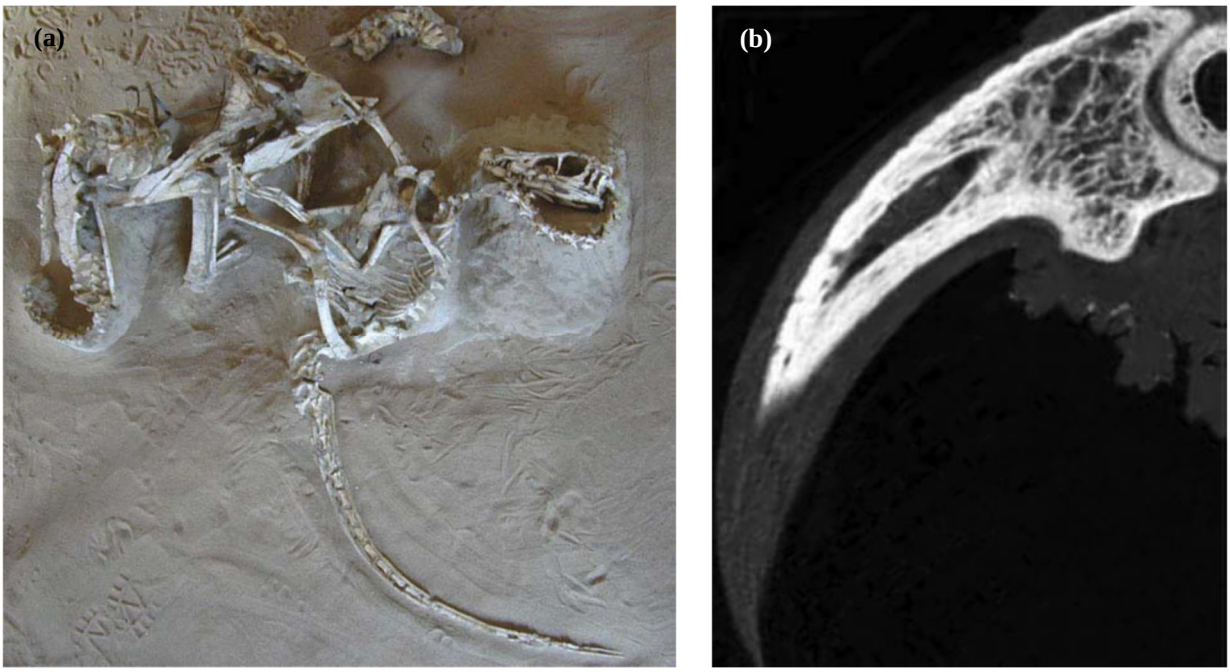

Fig. 8. Dromaeosaurid theropod dinosaur sample: (a) the ‘fighting pair’ Velociraptor and Protoceratops, and (b) high-resolution X-ray CT of owl terminal ungual phalanx and pedal claw (bone core and keratin sheath), where bone is white, keratin, and soft-tissue are grey [reprinted with permission from ref. 15].

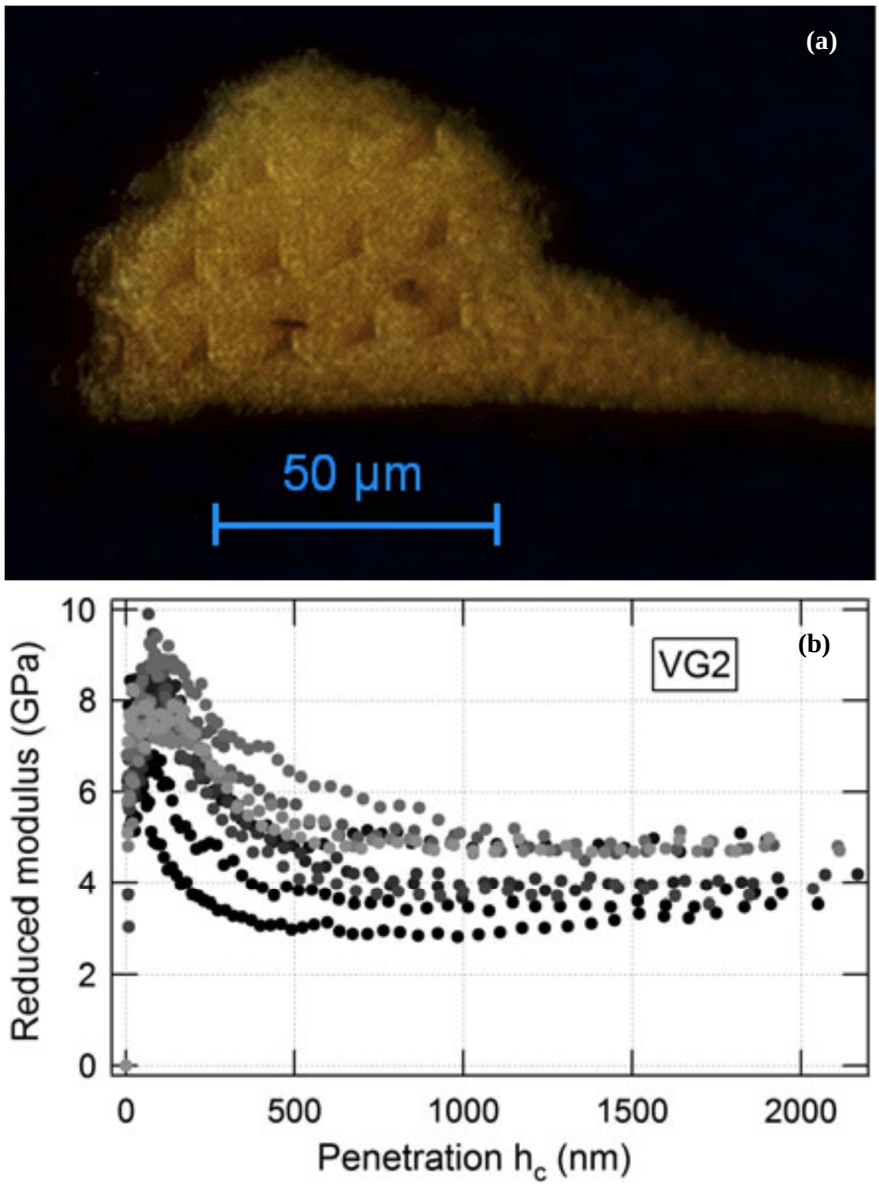

Fig. 9. (a) Optical microscope image of sample Van Gogh paintings (sample: VG2) after nanoindentation measurements, and (b) reduced elastic modulus as a function of penetration for ten measurements on sample VG2 [reprinted with permission from ref. 16] (Color figures online only).

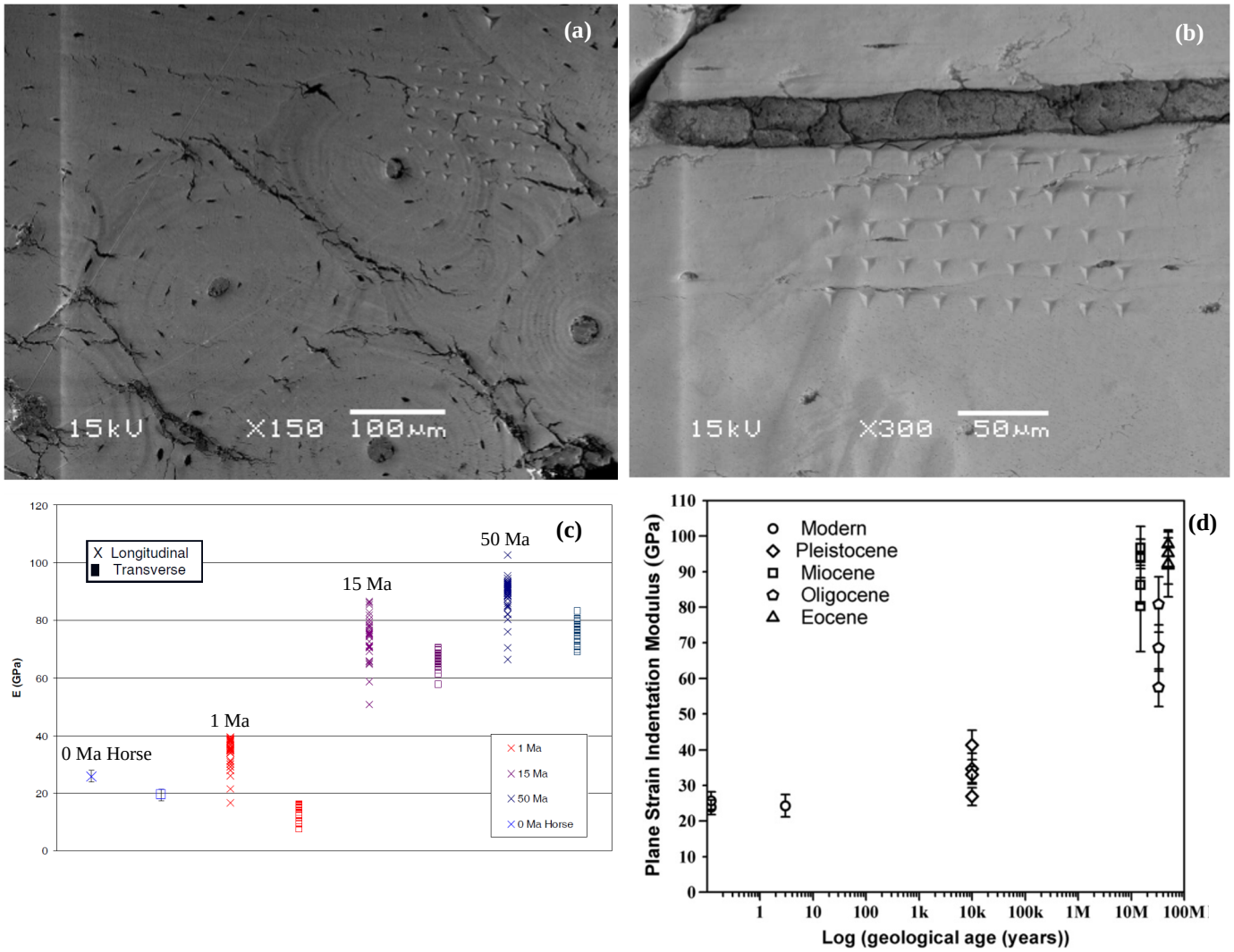

Fig. 10. Nanoindentation of fossilized and modern bone: (a) longitudinal axis 6x6 indent array over osteonal and interstitial bone, 15 Ma (million years ago) sample, (b) transverse axis 4x9 indent array starting at Haversian canal, 15 Ma sample, (c) cortical bone indents: longitudinal vs. transverse [reprinted with permission from ref. 17], and (d) longitudinal modulus values vs. the log of geological age (there is a clear increase of modulus values with the geologic age of the sample) [reprinted with permission from ref. 18] (Color figures online only).